Diffusion of single particles in cellular media

Victor Pereyra,[1,*] Andrey Milchev,[2] and Victor Fleurov[3]
[1]*Institut für Physik, Universität Mainz, D-55099 Mainz, Republic Federal of Germany*
[2]*Institute of Physical Chemistry, Bulgarian Academy of Sciences, 1040 Sofia, Bulgaria*
[3]*Beverly and Raymond Sackler School of Physics and Astronomy, Tel Aviv University, Tel Aviv 69978, Israel*
(Received 3 November 1993)

In this work we suggest a model for diffusion of particles in cellular media in which the walls of cells are characterized by strongly reduced permeability. Our analytical results are obtained for a regular system and confirmed also by extensive Monte Carlo simulations. They reveal several distinct regimes of diffusion behavior in time whereby an initially normal diffusion at very short times turns into a transient one at a characteristic crossover time τ_S and later, after a period marked by another characteristic time τ_L, returns to normal. At fixed permeability p of the cell walls we find that these crossover times scale as $\tau_S \propto L^2$ and $\tau_L \propto L$ with the cell size L, whereas for $L = \text{const}$ one has $\tau_L \propto p^{-1}$. These transitions from Gaussian to transient behavior are analyzed by cumulants of the mean quartic displacement $\langle x^4(t)\rangle$. Our results are valid for a regular arrangement of walls; however, we find generally that the course of the mean-square displacement $\langle x^2(t)\rangle$ with time is very similar to results obtained in the past for diffusion in disordered media. The frequency-dependent conductivity $\sigma(\omega)$ shows that at low frequency the real and imaginary parts of $\sigma(\omega)$ vary as ω^2 and ω, respectively, while saturating at constant values for $\omega \to \infty$. By measuring the dc and ac conductivity of charge carriers it becomes possible to determine both the size of the cells and the permeability of their walls.

PACS number(s): 05.60.+w, 66.30.−h, 05.40.+j

I. INTRODUCTION

Diffusion of particles in regular and disordered systems has been investigated extensively in recent years [1–11]. One of the most interesting features of stochastic transport predicted and observed in nonhomogeneous media is the (anomalous) non-Gaussian character of diffusive behavior. The understanding of the fundamentals of such a deviation from normal diffusive behavior is still a challenge from the point of view of basic research. It is also relevant for a number of applications, for instance, the ability of barrier materials to drastically resist the gas flux through them, the capacity of membranes for the separation of gases, etc. The transport of small molecules through *cellular media* could be ascribed to related problems of significant technological importance for a number of new materials, such as zeolites, soap froths, biological tissues, etc. Apart from the peculiarities of the periodicity structure and the form of the cells, one can view such cellular media as being composed of a more or less regular array of cavities, separated by walls. We may consider these cells as being filled by a homogeneous material so that the walker performs a conventional random walk before hitting the walls of the cage, which are characterized by some (reduced) permeability. The random walks are thus constantly disrupted by the interaction of the carrier with the cell walls and, as shown in the present paper, for certain values of the cell size L and the permeability of the walls p, the diffusive motion presents a crossover between two well characterized regions. Thus, during a transient period of time which may last many decades, the periodic system exhibits some characteristic features of transport in amorphous materials.

Much theoretical work has been done to elucidate the behavior of a single particle in disordered lattices [1–5]. There are also a number of studies considering the collective diffusion on homogeneous and heterogeneous substrates [6–10]. However, many aspects of the problem are still not understood completely.

In disordered systems such as glassy materials, polymers, etc., there are many difficulties in the characterization of the energy profile in which the particles are moving because energetic and topological disorder is not independent [11].

The lack of periodicity makes the problem difficult also for an analytical treatment and closed expressions have been derived in a few cases only. A number of results can be obtained as a series expansion [12] or numerically within the framework of the effective medium approximation [13,14] and also from renormalization group studies [15,16]. Another promising way to study the problem is through computer simulation using both Monte Carlo and molecular dynamics simulations, as, for example, in the dynamics of small molecules in dense polymers subject to thermal motion [17,18], tracer diffusion on random barrier media [19], tracer diffusion on heterogeneous surface [20,21], etc.

This paper presents a modified version of the dichotomic barrier model introduced by Haus *et al.* [22],

*Permanent address: INTEQUI, Universidad Nacional de San Luis-Chacabuco y Pedernera, 5700 San Luis, Argentina.

which is designed to describe motion in cellular materials. We consider the motion of a single particle in this cellular medium and calculate, by using the Monte Carlo simulation in one dimension (1D) and 2D and an analytical approach in 1D, several quantities related to the random walk performed by the particle, such as, for example, mean-square displacement, mean-quartic displacement, cumulants, etc. Some analytical results in 2D are also presented. We also calculate the frequency-dependent diffusion coefficient which allows for some conclusions concerning experimental measurements and structural characteristics of the systems.

We believe that the present model, in which an ordered system is shown to exhibit some features typical of anomalous diffusive behavior, provides an easy way to gain more insight into the mechanism of random walks in those interesting cases when diffusive behavior is not Gaussian.

The outline of this work is as follows. In Sec. I we introduce the model and general consideration. In Sec. II an analytical approach in one dimension is given and all the relevant quantities related to the random walk performed by the particles are calculated. In Sec. III we calculate the frequency-dependent diffusion coefficient and a general expression for both limits of high and low frequency is obtained as well as the correlation factor for jumps and a closed expression for the size of the cell. In Sec. IV we describe briefly the simulation scheme. In Sec. V we present the results and a discussion. Finally, a brief summary is given in Sec. VI. A brief analysis of the 2D problem is given in the Appendix.

II. MODEL

The cellular medium in our model is characterized by a regular array of cells which form an infinite lattice. The linear size L of these cells is given by the number of sites (potential wells) in which the walker may reside before jumping to a nearest neighbor site, separated from this by an energy barrier. We consider two possible values for the energy barriers between sites (a dichotomic barrier model) so that the probability to overcome the barrier has also two values Γ and Γ_p (see Fig. 1). The transition rate between sites within a cell is then given by Γ and the rate of crossing the cell borders by Γ_p. Since we generally assume that the cell walls are much more difficult for the walker to penetrate than the space within the cells, we assume that $\Gamma_p \ll \Gamma$. The high barriers are thought of as distributed periodically in space at distance $L+1$.

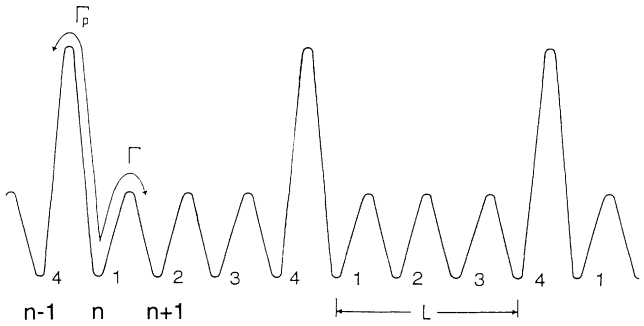

FIG. 1. Schematic representation of a cellular medium in 1D.

The motion of a random walker in such a periodic structure is described by the standard master equation

$$\frac{dP(\mathbf{n},t)}{dt} = \sum_{\langle \mathbf{n}',\mathbf{n}\rangle} W_{\mathbf{n}',\mathbf{n}}[P(\mathbf{n}',t) - P(\mathbf{n},t)] \,. \tag{1}$$

Here $P(\mathbf{n},t)$ is the conditional probability that the particle occupies site $\mathbf{n}$ after a time t has elapsed, given that it began at site $\mathbf{0}$ at $t=0$. The rates $W_{\mathbf{n}',\mathbf{n}}$ are assumed to be symmetric under an interchange of subscripts. The summation is over sites $\mathbf{n}'$, which are nearest neighbors of $\mathbf{n}$; this restriction in the summation being denoted by $\langle \mathbf{n}',\mathbf{n}\rangle$. We normalize for simplicity the values of the jump rates to that of the smaller barrier; then $\Gamma = 1/Z$ and $\Gamma_p = p/Z$, where Z is the number of nearest neighbors and p denotes the jump rate at which the particles overcome the higher barrier Γ_p.

III. ANALYTICAL SOLUTION IN 1D

In order to study the kinetics behavior of the particle it is necessary to solve Eq. (1). For simplicity, we can decompose the problem as follows.

Since all sites within a given cell are not equivalent (see Fig. 1), let us define the conditional probability $P_j(n,t)$ such that the position of the particle (measured from the origin) at time t be n, given that its relative position within the cell is j ($j = 1, 2,...,$L). It is then clear that

$$P(\mathbf{n},t) = \sum_{j=1}^{L} P_j(n,t). \tag{2}$$

The master equation (1) can be rewritten as a set of L coupled differential equations as

$$\begin{aligned}
\frac{dP_1(n,t)}{dt} &= -\frac{(1+p)}{2}P_1(n,t) \\
&\quad + \frac{1}{2}P_2(n+1,t) + \frac{p}{2}P_L(n-1,t) \,, \\
\frac{dP_j(n,t)}{dt} &= -P_j(n,t) + \frac{1}{2}P_{j-1}(n-1,t) \\
&\quad + \frac{1}{2}P_{j+1}(n+1,t) \,, \qquad (3) \\
\frac{dP_L(n,t)}{dt} &= \frac{p}{2}P_1(n+1,t) \\
&\quad + \frac{1}{2}P_{L-1}(n-1,t) - \frac{(1+p)}{2}P_L(n,t) \,.
\end{aligned}$$

After the set of equations (3) is Fourier and Laplace transformed, we obtain the following set of algebraically coupled equations for the Fourier-Laplace transform $\mathcal{L}_j$ of the probability P_j:

$$\left[s+\frac{(1+p)}{2}\right]\mathcal{L}_1(k,s)-\frac{e^{-ik}}{2}\mathcal{L}_2(k,s)$$

$$-\frac{pe^{ik}}{2}\mathcal{L}_L(k,s)=\mathcal{F}_1(k,0)\ ,$$

$$-\frac{e^{ik}}{2}\mathcal{L}_{j-1}(k,s)-(1+s)\mathcal{L}_j(k,s)$$

$$-\frac{pe^{-ik}}{2}\mathcal{L}_{j+1}(k,s)=\mathcal{F}_j(k,0)\ , \quad (4)$$

$$-\frac{pe^{-ik}}{2}\mathcal{L}_1(k,s)-\frac{e^{ik}}{2}\mathcal{L}_{L-1}(k,s)$$

$$-\left[s+\frac{(1+p)}{2}\right]\mathcal{L}_L(k,s)=\mathcal{F}_L(k,0)\ .$$

The initial conditions are $\mathcal{F}_j(k,0)=1/L$, i.e., the particle has the same probability of starting from any type of lattice site. We can write (4) in a compact form as

$$\mathbf{M}_L\cdot\mathbf{L}_L=\mathbf{F}_L(0)\ , \quad (5)$$

where

$$\mathbf{L}_L(k,s)=\begin{pmatrix}\mathcal{L}_1(k,s)\\ \vdots\\ \mathcal{L}_j(k,s)\\ \vdots\\ \mathcal{L}_L(k,s)\end{pmatrix} \quad (6)$$

and

$$\mathbf{F}_L(k,0)=\begin{pmatrix}\mathcal{F}_1(k,0)\\ \vdots\\ \mathcal{F}_j(k,0)\\ \vdots\\ \mathcal{F}_L(k,0)\end{pmatrix} \quad (7)$$

and the matrix $\mathbf{M}_L$ is given by

$$\mathbf{M}_L(k,s)=\begin{pmatrix}\left[s+\frac{(1+p)}{2}\right] & -\frac{e^{-ik}}{2} & \cdots & 0 & \cdots & -\frac{pe^{ik}}{2}\\ -\frac{e^{ik}}{2} & [1+s] & -\frac{e^{-ik}}{2} & 0 & \cdots & 0\\ 0 & -\frac{e^{ik}}{2} & [s+1] & -\frac{e^{-ik}}{2} & \cdots & 0\\ \cdots & \cdots & \cdots & \cdots & \cdots & \cdots\\ -\frac{pe^{-ik}}{2} & \cdots & 0 & \cdots & -\frac{e^{ik}}{2} & \left[s+\frac{(1+p)}{2}\right]\end{pmatrix}\ . \quad (8)$$

In order to solve the set of equations (5) we have to determine the eigenvalues of $\mathbf{M}_L$. In fact this matrix can be expressed via simpler tridiagonal matrices $\mathbf{B}_L$

$$\mathbf{B}_L(k,s)=\begin{pmatrix}[s+1] & -\frac{e^{-ik}}{2} & \cdots & 0 & \cdots & 0\\ -\frac{e^{ik}}{2} & [s+1] & -\frac{e^{-ik}}{2} & 0 & \cdots & 0\\ \cdots & \cdots & \cdots & \cdots & \cdots & \cdots\\ 0 & \cdots & \cdots & -\frac{e^{ik}}{2} & [s+1] & -\frac{e^{-ik}}{2}\\ 0 & \cdots & 0 & \cdots & -\frac{e^{ik}}{2} & [s+1]\end{pmatrix}\ . \quad (9)$$

For the determinants of these matrices one gets the relation

$$\mathrm{Det}\mathbf{M}_L=\left[s^2+s(p+1)+\frac{p}{2}\right]\mathrm{Det}\mathbf{B}_{L-2}-\frac{(p+s)}{4}\mathrm{Det}\mathbf{B}_{L-3}-\frac{p\cos(Lk)}{2^{L-1}}\ , \quad (10)$$

where for $\mathrm{Det}\mathbf{B}_L$ the following recurrence relation holds:

$$\mathrm{Det}\mathbf{B}_L=(s+1)\mathrm{Det}\mathbf{B}_{L-1}-\frac{\mathrm{Det}\mathbf{B}_{L-2}}{4}\ . \quad (11)$$

Here $\mathrm{Det}\mathbf{B}_0 = 1$ and $\mathrm{Det}\mathbf{B}_j = 0$ for $j < 0$. The recurrence (11) can be resolved since the matrix $\mathbf{B}_L(s)$ can be diagonalized as

$$\mathrm{Det}\mathbf{B}_L(s) = \prod_{j=1}^{L} \left[1 + s - \cos\left(\frac{j\pi}{L+1}\right)\right] . \tag{12}$$

Now we can use the identity [23]

$$\prod_{j=1}^{L} \left[\frac{(1+x^2)}{2x} - \cos\left(\frac{j\pi}{L+1}\right)\right] = \frac{x^{2(L+1)} - 1}{(x^2-1)2^L x^L} , \tag{13}$$

where x must satisfy $x^2 - 2(s+1)x + 1 = 0$. Then we obtain the general expression in the form

$$\mathrm{Det}\mathbf{B}_L(s) = \frac{\{1 + s + [(1+s)^2 - 1]^{1/2}\}^{2(L+1)} - 1}{2^L\{1 + s + [(1+s)^2 - 1]^{1/2}\}^L\{(1 + s + [(1+s)^2 - 1]^{1/2})^2 - 1\}} , \tag{14}$$

where $\mathrm{Det}\mathbf{B}_L \to (L+1)/2^L$ for $s \to 0$. Thus Eq. (10) may be written as an Lth-order polynomial in powers of s

$$\frac{2L(1-p+pL)}{2^L}s + \frac{L(L^2-1)(2-2p+pL)}{3\times 2^L}s^2$$

$$+\frac{L(L^2-1)(L^2-4)(3-3p+pL)}{45\times 2^L}s^3 + \cdots$$

$$+\frac{2p}{2^L}[1 - \cos(Lk)] = 0 . \tag{15}$$

It is thus evident from Eq. (15) that for $k = 0$ there is always an eigenvalue $s = 0$ which guarantees that the probability of finding the walker at times $t \to \infty$, infinitely far away from where it has started, is finite. The analysis of the L eigenvalues which emerge for the case of a cell with L sites shows that they oscillate with a period of $\frac{2\pi}{L}$ within the interval $[-2 < s < 0]$ forming bands of width $\approx p$. The smallest eigenvalue of Eq. (11), which determines the long time behavior of the tracer particle is found in the limit $k \to 0$

$$s_0 = -\frac{pLk^2}{2[1 + p(L-1)]} . \tag{16}$$

As is well known [1] (15) yields the diffusion coefficient at large ($t \to \infty$) times, which for our model appears to be

$$D_{t=\infty} = \frac{pL}{1 + p(L-1)} . \tag{17}$$

As we can see in Eq. (17), the diffusion coefficient always depends on the product of the two parameters of our model, namely, the probability p and the size of the cell L. For $p \to 0$ also $D_{t=\infty} \to 0$, i.e., all particles will be confined within the cells with impenetrable walls. For the physically interesting case $pL \ll 1$ one would expect thus that for a finite p the diffusion coefficient will be linearly proportional to the cell size L. It is worthwhile to mention here that this result would hold also for a disordered system if it can be characterized by an average cell size L. However, one should be more cautious when considering frequency-dependent conductivity in disordered systems.

The second smallest eigenvalue s_1 of $\mathbf{M}_L$ is expected to determine the slowest relaxation time of the diffusive behavior back to normal. An estimate of the dependence of this relaxation time on cell size $L > 4$ may be derived from Eq. (15)

$$s_1 = -\frac{6(1-p+pL)}{(2-2p+pL)(L^2-1)} \approx -\frac{3}{L^2} , \tag{18}$$

which scales proportionally to L^2. The exact values for the first few cell sizes are $s_1 = -(1+p)$ for $L = 2$, $s_1 = -(1+2p)/2$ for $L = 3$, and $s_1 = (-2 - p + \sqrt{2+2p+p^2})/2$ for $L = 4$. Since the eigenvalues are distributed symmetrically with respect to -1 in the interval $[-2, 0]$, the respective *largest* eigenvalues, which influence the initial deviation from the normal diffusive behavior, are given simply by $-2 - s_1$. Thus one may conclude that all relaxation times of the system scale proportionally to L^2. In Fig. 2 this behavior of the relaxation times is ver-

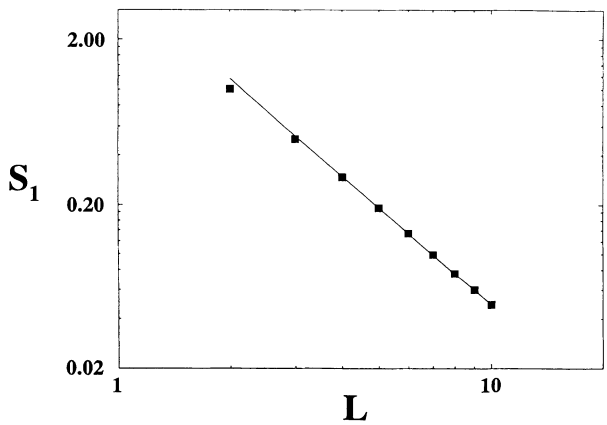

FIG. 2. Dependence of the second smallest eigenvalue s_1 on cell size L.

ified for the case of the second smallest eigenvalue s_1 for $2 < L < 10$. Due to the comparatively small values of L, the slope of this dependence is somewhat less than 2 (≈ 1.967). We shall see later that s_1 plays an important role in the frequency-dependent diffusion coefficient.

By solving Eqs. (4) and using (2) with the initial condition we can get $\mathbf{L}(k,s)$ and obtain the mean-square displacement and the mean-quartic displacement as a function of s or t

$$\langle x^2(s)\rangle = -\left.\frac{\partial^2 \mathbf{L}(k,s)}{\partial k^2}\right|_{k=0} \tag{19}$$

and

$$\langle x^2(t)\rangle = -\left.\frac{\partial^2 \mathbf{F}(k,t)}{\partial k^2}\right|_{k=0} \tag{20}$$

and similarly for the mean quartic displacement we have

$$\langle x^4(s)\rangle = \left.\frac{\partial^4 \mathbf{L}(k,s)}{\partial k^4}\right|_{k=0} \tag{21}$$

and

$$\langle x^4(t)\rangle = \left.\frac{\partial^4 \mathbf{F}(k,t)}{\partial k^4}\right|_{k=0} . \tag{22}$$

It seems instructive to show the final expression for $\mathbf{L}(k,s)$ at least for $L = 2, 3$. For $L = 2$ we have

$$\mathbf{L}_2(k,s) = \frac{s + (1+p)[1+\cos(k)]/2}{s^2 + s(1+p) + p[1-\cos(2k)]/2} \tag{23}$$

and similarly for $L = 3$,

$$\mathbf{L}_3(k,s) = \frac{s^2 + s(2+p)[2+\cos(k)]/3 + (1+2p)[\frac{\cos(k)}{3} + \frac{\cos(2k)}{6} + \frac{1}{4}]}{s^3 + (p+2)s^2 + 3(1+2p)s/4 + p[1-\cos(3k)]/4} . \tag{24}$$

Now using Eq. (19) we can obtain the mean-square displacement as a function of s, as

$$\langle x_2^2(s)\rangle = \frac{s(1+p) + 4p}{2s^2(1+p+s)} \tag{25}$$

for $L = 2$,

$$\langle x_3^2(s)\rangle = \frac{2s(2+p) + 9p}{3s^2(1+2p+2s)} \tag{26}$$

for $L = 3$, and

$$\langle x_4^2(s)\rangle = \frac{2s^2(3+p) + 2s(5+4p) + 16p}{4s^2(1+3p+4s+2ps+2s^2)} \tag{27}$$

for $L = 4$.

We can also get the time dependence of the mean-square displacement by using inverse Laplace transforms. Here we present only the analytical results of this procedure for $L = 2$,

$$\langle x_2^2(t)\rangle = \frac{1}{2}\left[\frac{p-1}{p+1}\right]^2 (1 - e^{-(1+p)t}) + \frac{2pt}{(1+p)} , \tag{28}$$

and for $L = 3$,

$$\langle x_3^2(t)\rangle = \frac{4}{3}\left[\frac{p-1}{2p+1}\right]^2 (1 - e^{-\frac{(1+2p)t}{2}}) + \frac{3pt}{(1+2p)} . \tag{29}$$

For larger systems we obtain the time dependence of $\langle x^2(t)\rangle$ numerically. It is seen from Eqs. (28) and (29) that the deviations from purely diffusive behavior, represented by the first terms on the right-hand sides of (28) and (29), vanish exponentially with time, provided $p < 1$. The relaxation times are indeed given by s_1. For $p = 1$ one has $\Gamma = \Gamma_p$, i.e., the cell borders are equally permeable as the inner space and diffusion is normal. In the coefficient of the linear terms on the right-hand side of (28) and (29) one easily recovers the general result (17).

IV. FREQUENCY DEPENDENCE OF THE DIFFUSION COEFFICIENT

The diffusion coefficient $D(\omega)$ at frequency ω is given by the following equation [24]:

$$D(\omega) = -\omega^2 \int_0^\infty \langle x^2(t)\rangle e^{-i\omega t} dt \tag{30}$$

and related to the conductivity $\sigma(\omega)$ by the generalized Einstein relation

$$\sigma(\omega) = \frac{\mathcal{N} e^2 D(\omega)}{k_B T} , \tag{31}$$

where $\mathcal{N}$ is the density of effective carriers of charge e, k_B is the Boltzmann factor, and T is the temperature. The conductivity $\sigma(\omega)$ depends only on equilibrium properties of the system in the absence of an applied electric field.

We can insert Eqs. (28) and (29) into (30) to obtain $D(\omega)$ for $L = 2$,

$$D(\omega) = \frac{2p}{(1+p)} + \frac{(p-1)^2\omega^2}{2(p+1)[\omega^2 + (1+p)^2]} + i\frac{\omega(p-1)^2}{2[\omega^2 + (1+p)^2]} , \tag{32}$$

and for $L = 3$,

$$D(\omega) = \frac{3p}{(1+2p)} + \frac{2(p-1)^2\omega^2}{3(2p+1)[\omega^2+(1+2p)^2/4]}$$

$$+i\frac{\omega(p-1)^2}{3[\omega^2+(1+2p)^2/4]} \,. \tag{33}$$

This frequency dependence of D underlines the distinction of our model from the case of normal diffusion where $D(\omega) = \text{const}$. Again the condition for this is $p < 1$. In Fig. 3 we show $\mathrm{Re}D(\omega)$ and $\mathrm{Im}D(\omega)$ for $L = 4$. Evidently, with growing ω the real part of the diffusion coefficient initially increases quadratically with ω and then at higher ω saturates at a new value, different from the low-frequency limit. It is interesting to note that this frequency dependence $\mathrm{Re}\sigma(\omega) \propto \omega^2$ is similar to the dominant behavior obtained in the case of electrons hopping between localized eigenstates in a disordered system at very low temperatures [25–27]. The imaginary part changes linearly with ω at low frequencies, and goes as ω^{-1} at high frequencies thus vanishing in the limit $\omega \to \infty$. In between $\mathrm{Im}D(\omega)$ has a maximum (cf. Fig. 3) which gets sharper with growing L. It can be inferred from Eqs. (32) and (33) that the exact position of this peak is determined by $\omega = s_1$.

A general expression for the low- and the high-frequency $D(\omega)$ for arbitrary L and p may be derived even more easily from $s^2\langle x^2(t)\rangle$, Eqs. (25)–(27), in the limits $s \to 0$ and $s \to \infty$. Thus one readily recovers the old result (17) for the static diffusion coefficient

$$D_0 = D(\omega \to 0) = \frac{Lp}{1+(L-1)p} \,, \tag{34}$$

whereas for large ω ($\omega \to \infty$) we obtain the high-frequency limit

$$D_\infty = D(\omega \to \infty) = \frac{L-1+p}{L}. \tag{35}$$

One may introduce here also the correlation factor f as a proportionality constant

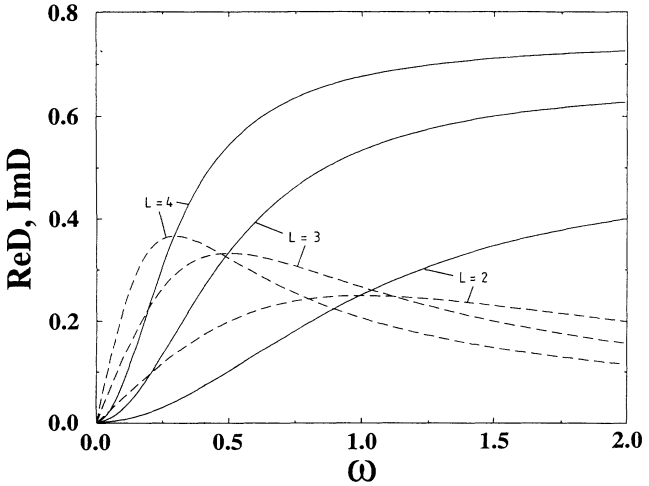

FIG. 3. Dependence of the real (solid line) and imaginary (dashed line) diffusion coefficient on frequency ω.

$$D_0 = fD_\infty \tag{36}$$

and measure the degree of correlation between successive hops of the particle. Here one gets

$$f = \frac{pL^2}{(L-1+p)[(L-1)p+1]}. \tag{37}$$

Evidently for $Lp \ll 1$ we have $f \approx Lp$, whereas for sufficiently large L and $Lp > 1$ most of the hops are uncorrelated as $f \to 1$.

In the major part of our results so far the two governing parameters of our model L and p have appeared as a product Lp. It is thus difficult to extract structural features of the medium on the ground of transport measurements of static properties alone. In this respect Eqs. (34) and (35) are important from an experimental point of view since with these two relations it is possible to determine separately L (the size of the cells) and p (the limiting jump probability) from the experimental measurements of D_0 and D_∞ as

$$L = \frac{D_0D_\infty - 2D_0 + 1}{D_0D_\infty - D_0 - D_\infty + 1} \,. \tag{38}$$

It is interesting to note that for $p = 1$ (i.e., the cells have no "volume") we get from Eq. (37) $D_0 = D_\infty$ and it is not possible to determine L, i.e., $p = 1$ reduces all results to the case of normal diffusion. In order to know p for a given L one has to solve a quadratic equation, which follows from (32) and (33), where only the real roots have physical meaning. Without solving it we give here only the condition for this

$$(1+D_0D_\infty)^2 + 4D_0^2 > 4(D_0 + D_0^2D_\infty). \tag{39}$$

For Lp fixed ≈ 1 we have $D_0 < D_\infty \leq 1$ and the system has always meaningful solutions. It can be proved that for reasonable values of D_0, D_∞ (39) is always fulfilled.

V. MONTE CARLO SIMULATION SCHEME

This section describes briefly the simulation procedure which was used to test our analytical predictions. Calculations are performed on 1D and 2D square lattices. As described above, we consider an infinite cellular system, that is, a replica of an $L \times L$ lattice, where the border sites are connected with probability p to the next lattice. Then a simple random walk is performed and the usual quantities are stored: $\langle x^2(t)\rangle$, $\langle x^4(t)\rangle$, $P(\mathbf{n},t)$, and the fourth-order cumulant C_L defined as

$$C_L = 1 - \frac{\langle x^4(t)\rangle}{3\langle x^2(t)\rangle^2}. \tag{40}$$

The last quantity is used to test whether the distribution $P(\mathbf{n},t)$ is Gaussian or not, since for a Gaussian distribution $C_L \equiv 0$.

A trial move is carried out as follows: (i) A site $\mathbf{n}$ in the lattice is chosen at random and is considered as a starting point and (ii) the probability $W_{n',n}$ is compared

with a random number and the time is increased by one unit whether or not the jump is successful. If the jump is rejected, then another direction is chosen at random. The usual averages are taken over 10^5 runs and the length of each run is 10^5 Monte Carlo steps. In the simulation the size of the unit cell varies from $L = 2$ to 80.

VI. RESULTS AND DISCUSSION

Figure 4 shows the behavior of the mean-square displacement in 1D, for fixed p ($p = 0.001$) and different sizes of the unit cell ($L = 2$–80), where the symbols denote the Monte Carlo results and the full lines correspond to the analytical functions, Eqs. (29) and (30) for $L = 2, 3$, and the numerical inverse Laplace transform results of Eq. (28) for $L = 4$. Evidently one observes excellent agreement between the analytic prediction and the computer experiment. Following the curves in Fig. 4, we can distinguish three time regimes: (i) a short initial period when the walker is expected to move in a finite "cage" of size L^d (d = dimension) before it hits its walls (during this interval we observe, especially for large L, a quasinormal diffusion as long as $x^2 < L^2$), (ii) a transient time interval when the motion is clearly subdiffusive and lasts rather long depending on the cell size L, and (iii) an asymptotic regime when the diffusion becomes eventually normal at later times.

In order to check the possibility to extend these results to higher dimensions we have carried out calculations for the quadratic regular cellular system with the cell size $L \times L$. This analytical calculation is much more involved than that presented above for the 1D system. However, the results for $L = 2$ and $L = 3$ are briefly described the Appendix. One can see from these equations as well as from the curves exhibited in Fig. 5 that the behavior of the mean-square displacement $\langle r^2(t) \rangle$ in 2D and the other characteristics of the system are similar qualitatively and in many aspects quantitatively (at long times) to the behavior of these characteristics in the 1D case. It is necessary here to emphasize an important difference between the behavior of a single particle in a regular array of barriers (where we can see a qualitative similarity between 1D and 2D) and anomalous diffusion where the mean-square displacement $\langle r^2(t) \rangle \propto t^\nu$, where ν depends on dimensionality and other details of the media (i.e., percolation exponents). In our model we have a crossover between two normal diffusion regimens; the three regimes are clearly separated by crossover times which are expected to depend on the basic parameters of our model L and p. In order to analyze the size dependence of the crossover times, we plot the first crossover time τ_S and the second crossover time τ_L as functions of the cell size (Fig. 6) for 1D and 2D. It is evident that both τ_S and τ_L scale with L. The slope for the first crossover time is

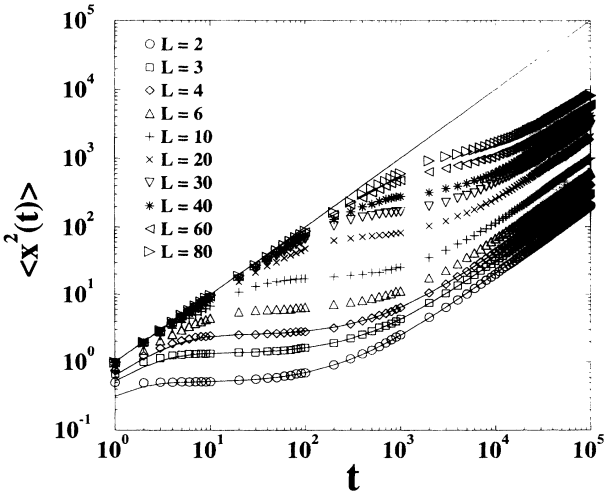

FIG. 4. Mean-square displacement vs time in 1D. The full lines correspond to analytical results and the symbols to Monte Carlo simulation.

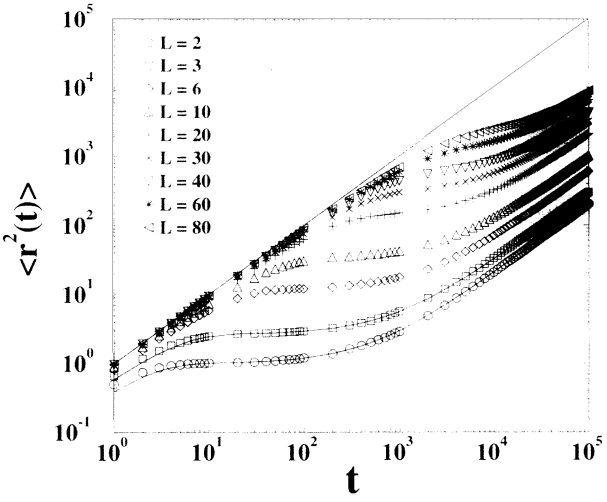

FIG. 5. Mean-square displacement vs time in 2D. The full lines correspond to analytical results and the symbols to Monte Carlo simulation.

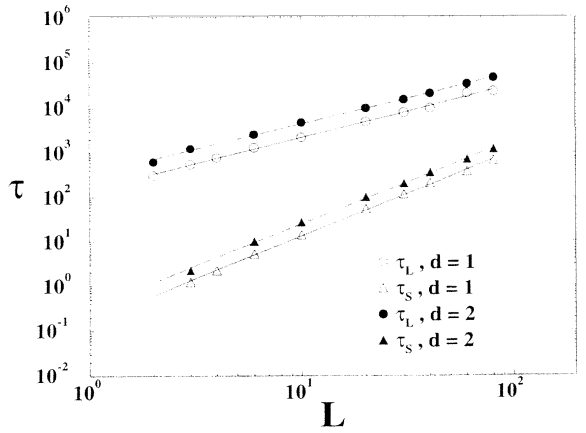

FIG. 6. Scaling behavior of the crossover times vs size of the cell.

nearly 2 (1.93), while the slope of the second crossover time is approximately 1 (1.13), independent of space dimension d. A simple analysis of these slopes suggests, for the first crossover time, that on the average the particle hits the border of the cell after a characteristic time τ_S that is proportional to L^2, during which period the motion is nearly normal. Exponential corrections to this behavior set in times proportional to L^2 [remember that all eigenvalues are proportional to L^{-2}; cf. Eq. (18)]. The second crossover time τ_L depends linearly on L and is expected to reflect the reduced diffusion coefficient because of the large barriers at the cell borders. Indeed, from Eq. (17) one has $D_{t=\infty} \approx pL$ for $pL \ll 1$ and this product determines the slope of the mean-square displacement in the large time limit. Generally one should also note that with the increasing cell size L at p =const the transient regime progressively vanishes and disappears at $pL \approx 1$. On the plots shown in Figs. 4 and 5 this happens at $L \approx 100$. The dependence of $\langle x^2(t) \rangle$ on t for various p is shown in Fig. 7 for $L = 6$ (this behavior is similar to the temperature dependence of $\langle r^2(t) \rangle$ on a correlated heterogeneous surface [21]). Again the intermediate subdiffusive regime may be detected as long as $pL < 1$. The corresponding p dependence of the large crossover time τ_L is shown in Fig. 8. We find that τ_L scales very nearly as L^{-1} (the slope in Fig. 8 is ≈ -0.94).

The most salient feature of the normal diffusion is the Gaussian character of the distribution function $P(\mathbf{n}, t)$. In order to analyze this characteristic of the distribution function we use the fourth-order cumulant defined in Eq. (40) [25]. The cumulant reflects sensitively the non-Gaussian character of the diffusion, since for normal diffusion $P(\mathbf{n}, t)$ is Gaussian and is well defined by its first and second moments (mean value and dispersion) as a consequence $C_L \equiv 0$. In Fig. 9 we show the fourth-order cumulants as a function of time for $L = 2, 3, 4$ and $p = 0.001$. Again both the analytical and Monte Carlo simulation results are in good agreement, except for very short times. The analysis of Fig. 9 shows that for $t \approx \tau_s$,

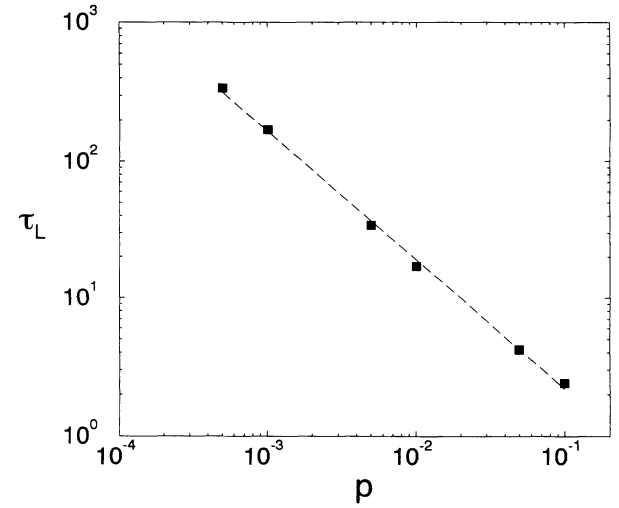

FIG. 8. Scaling behavior of the large crossover time τ_L vs p for $L = 6$.

C_L has a maximum and for $t \approx \tau_L$ a minimum, while eventually at very large time $t \to \infty$, $C_L \to 0$ and the distribution becomes Gaussian. In Fig. 10 we present, as an example, the evolution of the probability distribution function $P(\mathbf{n}, t)$ for these characteristic times (here $L = 10$ and $p = 0.001$). One can see that the distribution is always symmetric and finite and, as time increases, it eventually becomes Gaussian. In Fig. 11, we present the analytical results for the p dependence of the fourth-order cumulant for $L = 2$. We can see that as $p \to 1$, the cumulant $C_L \to 0$, even at very short times after the random walk has begun. An examination of the scaling behavior of the time τ_m (this is the time where the C_L has a minimum) as a function of p reveals (Fig. 12) that the slope of the curve is the same as in Fig. 8. Thus we conclude that the minimum of the curve C_L vs time corresponds to the large crossover time τ_L when the diffusive behavior turns from transient to normal.

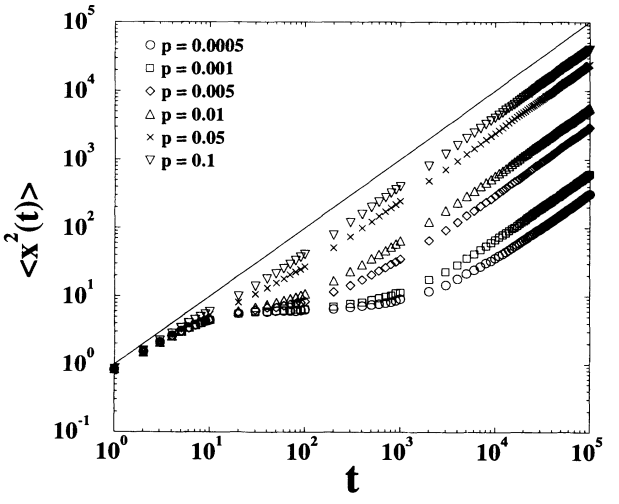

FIG. 7. Mean-square displacement vs time for $L = 6$ and different p.

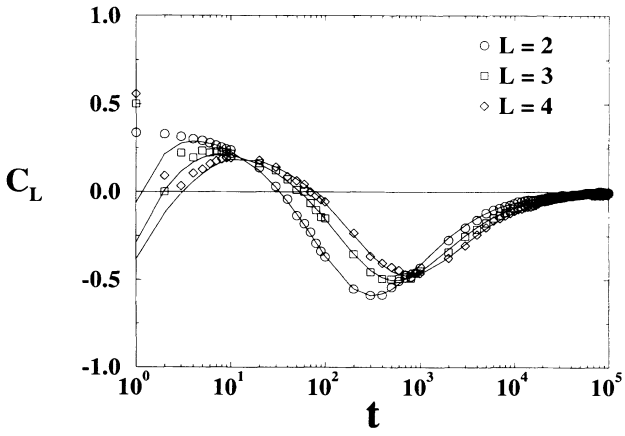

FIG. 9. Cumulants C_L for $L = 2, 3, 4$. Theory (lines) and simulations (symbols).

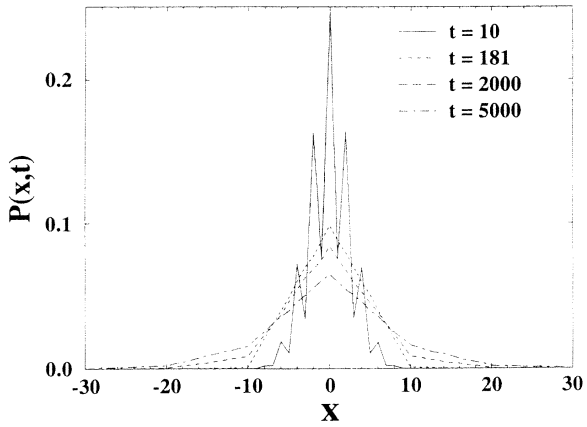

FIG. 10. Probability function for different times and $L = 10$.

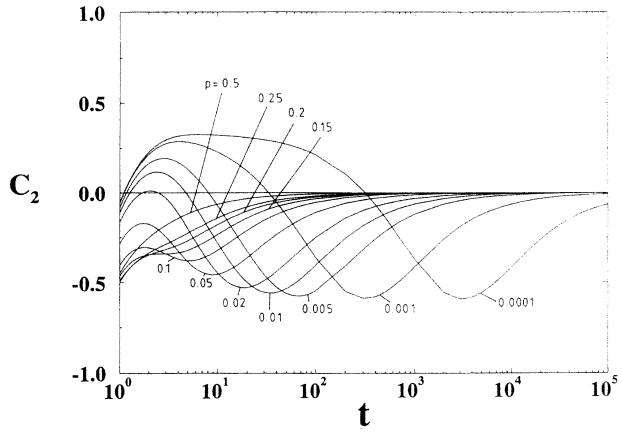

FIG. 11. Cumulants for $L = 2$ (theory) and different p.

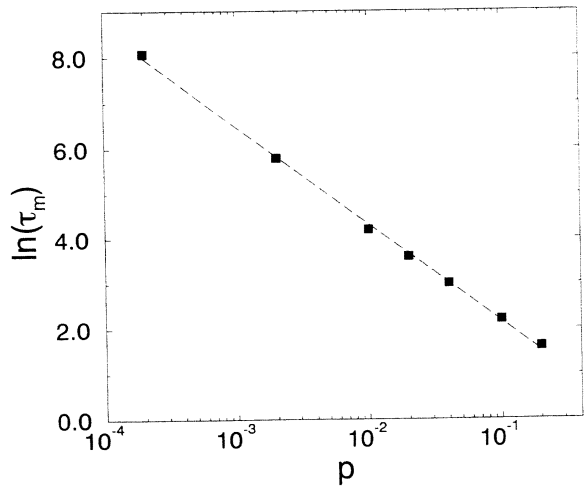

FIG. 12. Scaling behavior of the time τ_m vs p.

VII. SUMMARY AND FINAL COMMENTS

In this paper, we have presented both Monte Carlo simulations and exact calculations of the relevant quantities for the tracer diffusion in cellular structures. Mean-square displacement, quartic moments, and cumulants, as well as the frequency-dependent diffusion coefficient, have been calculated exactly in 1D for small cell sizes L. Some analytical results in 2D are presented in the Appendix. A general expression for the smallest eigenvalue which determines the long time behavior of the walker (diffusion coefficient at $t \to \infty$) has been obtained as a function of the size of the cell L and the permeability p. We also have calculated the second smallest eigenvalue, which determines the slowest relaxation time of the transient diffusive behavior back to normal. Our analysis reveals several distinct regimes of diffusive behavior in time where one observes an initial normal diffusion at very short times turning into a subdiffusive one at a characteristic crossover time τ_S and later, after a period determined by another characteristic time τ_L, returning to normal. We find that the smallest crossover times scale as $\tau_S \propto L^2$ and the largest crossover times scale as $\tau_L \propto L$, and we suggest an interpretation for this finding.

The non-Gaussian character of the diffusion at intermediate times is clearly seen from the fourth-order cumulant. Finally, we calculate the frequency-dependent diffusion coefficient and obtain a general expression for the low- and high-frequency limits of $D(\omega)$ for arbitrary L and p. As a consequence, it appears possible to obtain, by measuring the dc and the ac conductivity, closed expressions that determine both the size of the cells L and the permeability of the cell walls p. As emphasized frequently in the paper, a precondition for verification of these theoretical predictions is the requirement that $pL < 1$, since for $pL \approx 1$ diffusion becomes normal and no transient regimes whatsoever may be observed. The condition $pL < 1$ thus poses certain constraints on the combination of temperatures and cell sizes which can be investigated successfully.

As a final remark we should like to point out that the present model of a cellular medium as a periodic array of small and high barriers is not chosen arbitrary. We have checked that an alternative description in which barriers are replaced by traps, characterized by large mean stay times, i.e., the cell borders absorb the carriers which remain there for a long time before moving again into the next or the previous cell, leads to normal diffusive behavior at all time scales. Indeed, starting with a stationary distribution of tracer particles in shallow (ordinary) and deep (traps) sites and solving the governing set of equations (1) under the condition that jumps to the left or to the right from any site are symmetric produces a mean-square displacement changing linearly with time and the corresponding diffusion coefficient is given by Eq. (17). In fact the latter finding is not surprising since it has been rigorously proved [28] before that the mean-square displacement of a particle in the random-trap model is a linear function of time, provided that the initial probability distribution corresponds to a stationary distribution.

Given the observed deviations of diffusion behavior

from normal in real disordered systems, one may conclude that it is mainly the barrier component of the structure which is responsible for them.

ACKNOWLEDGMENTS

This work was supported by the CONICET, Argentine, the Deutsche Forschungsgemeinschaft under Grant No. 436-BUL-113/45, and the German-Israeli Foundation for Scientific Research and Development Grant No. I-140-125.7/89. The authors thank Professor K. Binder, Institute of Physics, Johannes Gutenberg University of Mainz, for the hospitality and useful discussion.

APPENDIX

The motion of a walker in a 2D cellular medium is considered, for example, on a regular square array of cells, each of them containing $L \times L$ sites. The probability p of crossing the border of such a cell is lower than the probability $1/4$ of jumping to one of the neighboring sites within the same cell. Let $P_j(n,m,t)$ be the probability that the walker occupies the site (n,m) with the label j ($j = 1,2,3,\ldots,L^2$), which gives the position within the cell. The motion of such a walker is described by a set of L^2 differential equations similarly to the 1D case considered in the main body of the text. It is rather difficult to deal with the corresponding matrices in the same general fashion as we did for the 1D case. However, the results for $L = 2,3$ can be obtained explicitly. For $L = 2$,

$$\langle r^2(s)\rangle = \frac{s(1+p)+2p}{s^2(1+p+2s)}$$

and in real time

$$\langle r^2(t)\rangle = \frac{3p+1}{p+1}[1-e^{-\frac{p+1}{2}t}] + \frac{2p}{p+1}t\ .$$

For $L = 3$,

$$\langle r^2(s)\rangle = \frac{4s(2+p)+9p}{3s^2(1+2p+4s)}$$

and

$$\langle r^2(t)\rangle = \frac{8}{3}\frac{1+p}{(1+2p)^2}[1-2^{-\frac{2p+1}{4}t}] + \frac{3p}{1+2p}t\ .$$

[1] J. W. Haus and K. W. Kehr, Phys. Rep. **150**, 263 (1987).
[2] S. Havlin and D. Ben-Avraham, Adv. Phys. **36**, 695 (1987).
[3] S. Alexander and R. Orbach, J. Phys. (Paris) **43**, L625 (1982); D. Ben-Avraham and S. Havlin, J. Phys. A **15**, L691 (1982).
[4] Y. Limoge and J. L. Bocquet, Phys. Rev. Lett. **65**, 60 (1990).
[5] J. P. Bouchard and A. Georges, Phys. Rep. **195**, 127 (1990).
[6] R. Kirchheim, Acta Metall. **35**, 271 (1987); R. Kirchheim and U. Stolz, *ibid.* **35**, 281 (1987)
[7] R. Gomer, Rep. Prog. Phys. **53**, 917 (1990).
[8] C. H. Mak, H. C. Anderson, and S. M. George, J. Chem. Phys. **88**, 4052 (1988).
[9] Y. Limoge and J. L. Bocquet, Acta Metall. **36**, 1717 (1988).
[10] A. Sadiq and K. Binder, Surf. Sci. **128**, 350 (1983).
[11] I. Avramov and A. Milchev, J. Non-Cryst. Solids **104**, 253 (1988).
[12] P. J. H. Denteneer and M. H. Ernst, J. Phys. C **16**, L961 (1983); Phys. Rev. B **29**, 1755 (1984).
[13] I. Webman and J. Klafter, Phys. Rev. B **26**, 5950 (1982).
[14] M. Sahimi, B. D. Huges, L. E. Scriven, and H. T. Davis, J. Chem. Phys. **78**, 6849 (1983).
[15] J. Matcha, J. Phys. A **18**, L531 (1985).
[16] A. E. Arinshtein and A. P. Moroz, Zh. Eksp. Teor. Fiz. **102**, 221 (1992) [Sov. Phys. JETP **75**, 117 (1992)].
[17] A. Gusev, S. Arizzi, U. Suter, and D. J. Moll, J. Chem. Phys. **99**, 2221 (1993); A. Gusev and U. Suter, *ibid.* **99**, 2228 (1993).
[18] F. Müller-Plathe, S. C. Rogers, and W. F. van Gunsteren, Chem. Phys. Lett. **199**, 237 (1992).
[19] I. Avramov, A. Milchev, and P. Argyrakis. Phys. Rev. E **47**, 2303 (1993).
[20] F. Bulnes, K. Sapag, J. Riccardo, V. Pereyra, and G. Zgrablich, J. Phys. Condens. Matter **5**, A223 (1993).
[21] K. Sapag, V. Pereyra, J. L. Riccardo, and G. Zgrablich, Surf. Sci. **295**, 433 (1993).
[22] J. W. Haus, K. W. Kehr, and K. Kitahara, Z. Phys. B Condens. Matter. **50**, 161 (1983)
[23] I. S. Gradsteyn and I. M. Ryzhik, in *Table of Integrals, Series and Products*, edited by A. Jeffrey (Academic Press, New York, 1980).
[24] H. Scher and M. Lax, Phys. Rev. B **7**, 4491 (1973); J. Heinrichs, *ibid.* **22**, 3093 (1980).
[25] T. Odagaki and M. Lax, Phys. Rev. B **24**, 5284 (1981).
[26] D. J. Thouless, Phys. Rep. C **13**, 93 (1974).
[27] E. A. Kaner and L. V. Chebotarev, Phys. Rep. **150**, 179 (1987).
[28] J. W. Haus, K. W. Kehr, and J. W. Lyklema, Phys. Rev. B **32**, 2905 (1982).